

# Numerical modeling of downlink electromagnetic wave exposure generated by 5G beamforming antennas

---

Nicolas Noé<sup>1</sup> and François Gaudaire<sup>2</sup>

<sup>1</sup>Lighting and Electromagnetism Division, CSTB, Nantes, France, nicolas.noe@cstb.fr

<sup>2</sup>Lighting and Electromagnetism Division, CSTB, Grenoble, France, francois.gaudaire@cstb.fr

---

**Keywords:** 5G, Antennas, Beamforming, Exposure

---

## Abstract:

In this paper different scenarios were compared for the numerical modeling of electromagnetic wave exposure to beamforming antennas. These scenarios range from the simplest (using an averaged radiation pattern) to an almost realistic one (MU-MIMO beamforming taking into account users locations) with intermediate ones. The results underline the influence of the environment around the antennas on the distribution of the electric field.

## 1 Introduction

The issue of EMF exposure to smart antennas was addressed for the first time under the angle of the security perimeters. Indeed, to respect the sanitary standards of exposure of workers, a security perimeter is established around the antenna, in which it is prohibited to intervene when the antenna is in operation. Usually this perimeter is determined by calculating the minimum distance around the antenna beyond which the electric field is always lesser than the legal threshold. This distance is evaluated in free space and hence only depend of the Equivalent Isotropic Radiated Power (EIRP).

For beamforming antennas, the antenna gain can vary dynamically up to a maximum gain when a beam is formed in a given direction. Hence using EIRP to compute security perimeters would lead to very high distance.

## 2 Previous work

In [1, 2, 3] a statistical approach was used to obtain adapted distances of security. The method used consisted in defining exposure scenarios, depending on a very limited number of parameters: cell type (macro or micro), number of users served simultaneously  $K$  and duration of service  $D$ . Users are randomly distributed in the environment (80% indoor, 20% outdoor) and the antenna behavior is simulated (at full load) for a given time (6 minutes) in order to obtain the probability distribution function (pdf) of the effective maximum gain. The cumulative density function of the maximum gain therefore only depends on the chosen parameters. As a consequence this allows to estimate, with a given probability, a safety distance for a maximum level of exposure.

## 3 New approach

The previous approach is perfectly suited for security perimeters, but it seems insufficient for quantifying public exposure in real environments. The question of exposure is not limited to safety limits concerns. One might indeed try to know precise local exposure (for the search for atypical points in France for example, or for compliance with much more restrictive local laws on the level of exposure such as in the Brussels-Capital region in Belgium). The local exposure may vary greatly depending on the actual configuration of the environment (layout of buildings, construction materials, ...), even for the same type of cell (macro or micro).

With the previous approach, an averaged diagram could be determined (as a complement to the maximum gain alone). This diagram can be used as an input to a detailed exposure simulation in a given environment, but it is likely that the simulation with the averaged diagram will give results different from the one that could be obtained by averaging the exposure over time.

We therefore propose a new approach to modeling of exposure to beamforming antennas, by studying several antenna modeling scenarios, from the simplest one to more and more complex ones. The main objective of this study is to compare an *a priori* statistical analysis (with an average diagram) with an *a posteriori* statistical analysis on these different scenarios.

## 4 Antenna, environments and simulation method

### 4.1 Antenna

The input antennas can either be a single point with a far field radiation pattern or a set of radiating sub-elements with to model a Uniform Planar Array (UPA) antenna with its beamforming capacity. The characteristics of the theoretical UPA antenna used in this study are:

- a 3GPP base element [4] with a 12.6 dBi gain, with a  $65^\circ$  horizontal aperture and a  $20^\circ$  vertical aperture,
- an  $8 \times 8$  array a elements with  $0.5\lambda$  horizontal spacing and  $0.6\lambda$  vertical spacing,
- beams that can be steered from  $-60^\circ$  to  $+60^\circ$  horizontally and from  $-20^\circ$  to  $+20^\circ$  vertically,
- a 24.8 dBi gain for a single beam and an input power of 52.04 dBm (160W).

Beamforming with this antenna is illustrated on figure 1. It must be noted that there are strong sides lobes for extreme azimuths (close to  $60^\circ$ ) since it is a purely analytical model and no side lobes suppression technique was applied.

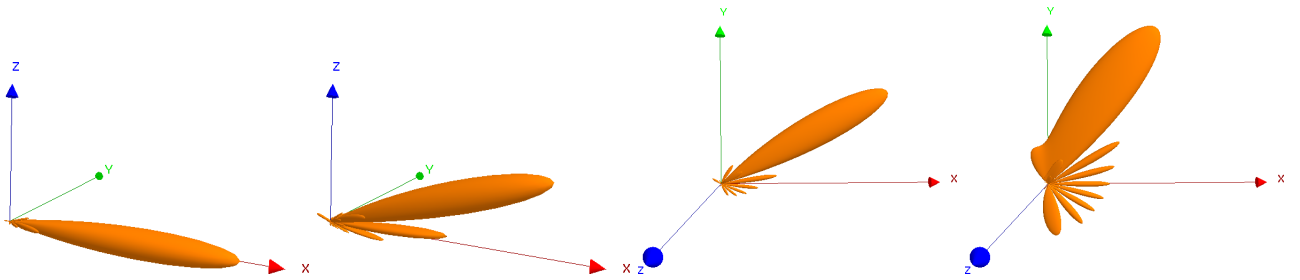


Figure 1 – Beamforming to azimuth & tilt (from left to right):  $0^\circ$  &  $0^\circ$ ,  $0^\circ$  &  $20^\circ$ ,  $30^\circ$  &  $0^\circ$ ,  $60^\circ$  &  $0^\circ$

## 5 Environments

Three environments have been studied. They are extract of a more complete Paris exposure simulation study and represent different configurations: one with mainly LOS exposure, one with other buildings reflections and a canyon street with indirect exposure. Only the buildings in the vicinity of the antenna have been kept (since only one antenna is used). The antenna is mechanically tilted  $3^\circ$  downward.

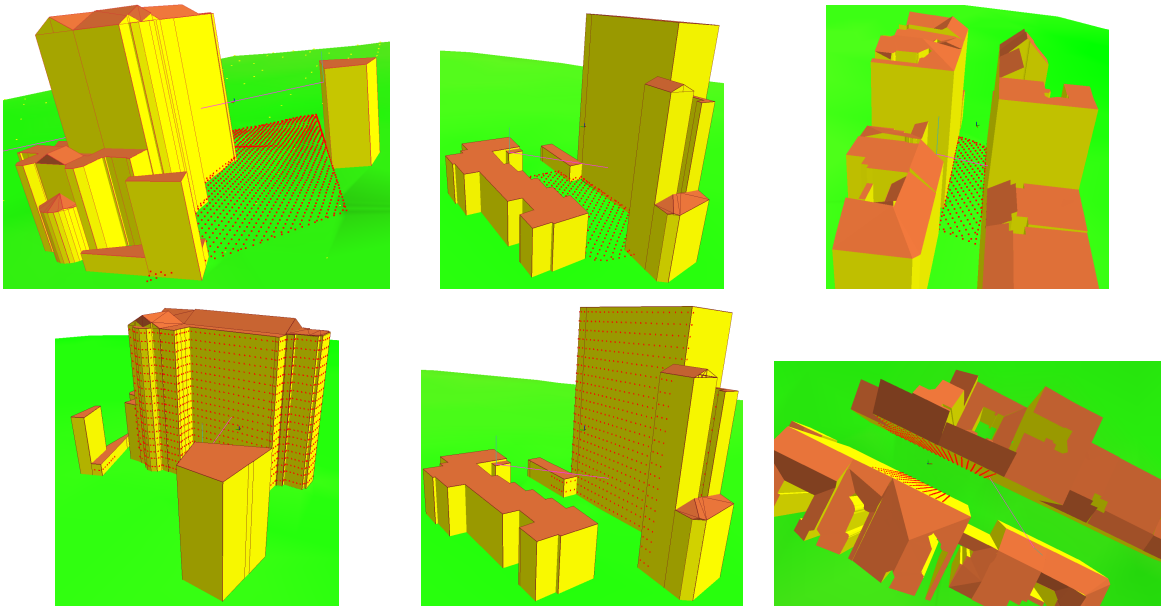


Figure 2 – First (left), second (middle) and third (right) environments: antenna with default main lobe direction, ground (top) and facade (bottom) maps

## 5.1 Simulation method

All simulations are performed using a 3D beam-tracing method [5]. This method computes paths between emitters and receivers, taking into account reflection, diffraction and transmission by obstacles, in order to get a complex electric field (with phase).

## 6 Scenarios

### 6.1 Scenario 0

For this scenario a single simulation is performed with an averaged (over all beam directions) far field diagram. This diagram has a 13.17 dBi gain and is illustrated on figure 3.

### 6.2 Scenario 0'

This scenario is related to the foreseen ANFR guidelines for 5G. It is a kind of envelop of all beams, made from the 3GPP base element with a  $120^\circ$  horizontal aperture and a  $40^\circ$  vertical aperture and an (artificial) gain of 24.3 dBi. Once again a single simulation is performed with this diagram and then a 13.5 dBi loss factor (from ANFR guidelines, to account for 5G usage) is applied to the final result. This diagram is illustrated on figure 3.

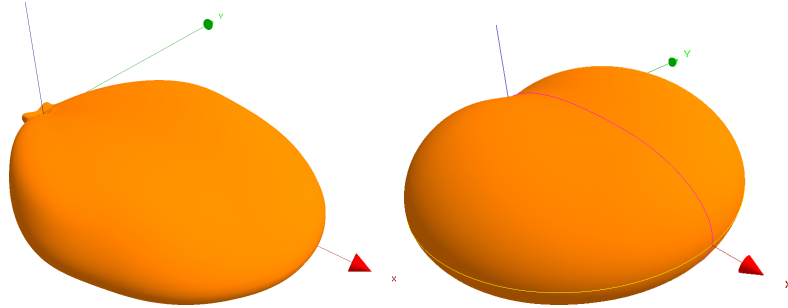


Figure 3 – Far field diagrams (linear) used for scenarios 0 (left) and 0' (right)

### 6.3 Scenario 1

In this scenario, beams are formed in every possible direction (whatever the environment is). One simulation is performed with a radiation pattern for each beam direction, with a  $1^\circ$  sampling (hence 4961 simulations and exposure maps) as illustrated on figure 4. Then an average exposure map is computed to compare to other scenarios.

### 6.4 Scenario 1'

With a smart antenna it is hinted that beams are formed only in directions where users really stand. A rough approximation is to consider only beams pointing to exposure points (either on the ground or on the building frontages) that are in line-of-sight of the antenna. As a matter of fact users are either in the streets or in the building, and not floating in air yet. The main point of this scenario is that it is easy to set up without any change in simulation tools, as it is only a sub-case of scenario 1. For the studied environments, LOS exposure points represent 10% of the ground surface and 20% of the facades (mainly the building in front of the antenna) as illustrated on figure 4.

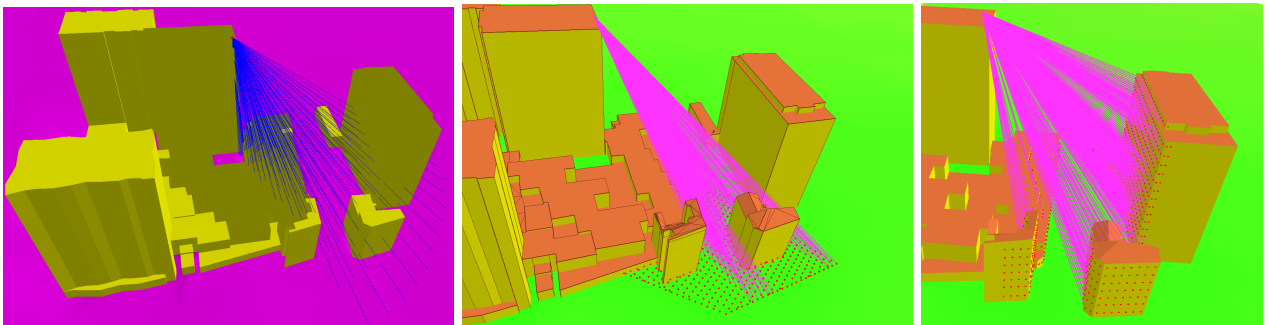


Figure 4 – Scenario 1 (left, beams in all possible directions), scenario 1' (middle and right, beams towards LOS exposure points on the ground and on the facades)

## 6.5 Scenario 2

In this scenario, users are taken into account and beamforming is dynamically computed depending on the channel between the antennas sub-elements and the users. It aims at reproducing the real behaviour of a MU-MIMO antenna.

### 6.5.1 Users

A pool of user equipments (UEs) is created. UEs are randomly distributed on the ground and inside the buildings with a ratio (for the same footprint) of 80% indoor UEs and 20% outdoor UEs. There are far more UEs in this pool than real users, in order to represent moving UEs and changing reception conditions. In this study 640 UEs were generated (540 indoor, 100 outdoor), see figure 5.

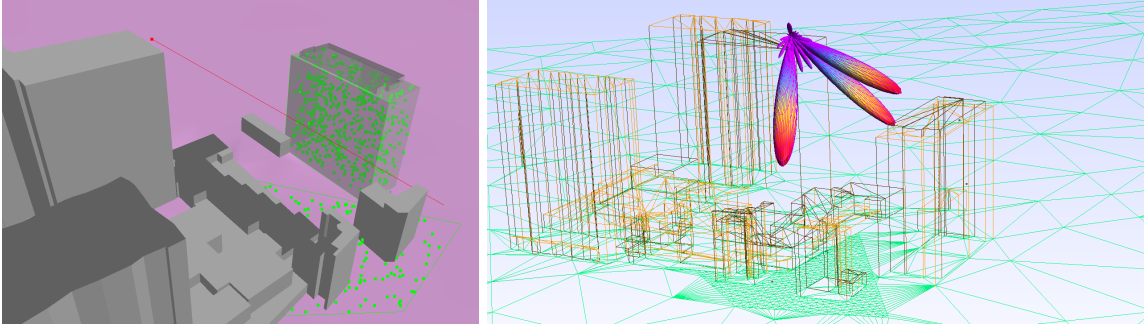


Figure 5 – Scenario 2’: randomly generated UEs (left) and MU-MIMO beamforming for  $K=3$  served UEs (right)

### 6.5.2 Beamforming

In this study we used zero-forcing beamforming [6]. It aims at maximizing the SINR (signal to interference and noise ratio) so as to serve a maximum number of UEs simultaneously. The beamforming weights are obtained by computing the pseudo-inverse of the channel matrix between the 64 sub-elements of the antenna and a set of  $N$  UEs ( $N \leq 64$ ). The channel matrix is computed with the simulation method (each channel being the result of multiple paths contributions).

A greedy user selection is done to find the number  $K$  of UEs that can be served simultaneously amongst the  $N$  UEs with the overall higher rate with a given noise. Power allocation between users is done with a water-filling method. Actually  $K$  is not a parameter here, as it is automatically computed (usually 3 or 4).

### 6.5.3 Full algorithm

- UEs are handled by batches of 64 UEs. First these 64 UEs are removed from the pool of UEs (keeping the ratio between indoor and outdoor UEs, hence 50 indoor UEs and 14 outdoor UEs). Beamforming is performed on the 64 UEs by successive iterations, until every UE has been served (each UE has the same drop duration  $D$ ). Hence for each iteration  $i$  of beamforming,  $K_i$  UEs are served, with their allocated power. An exposure map is computed for each iteration, corresponding to the full antenna power.
- Once the 64 UEs have served, 64 others are extracted from the pool and so one, until the pool empties.
- When the pool is empty, an averaged (over the total number of iterations and also over time since  $D$  is constant) exposure map is computed.

The downlink rate for each UEs is computed but is not used yet.

## 7 Preliminary results

First we compare scenarios 0 (map with averaged diagram) and 1 (average of maps for each diagram). As expected the mean error between them is very close to zero. Nevertheless the error on some isolated points can be quite high. For instance the interference (either constructive or destructive) between direct and reflected field is amplified in scenario 0 due to the not very directional diagram. For instance on five highly exposed points (expressed in V/m):

| point      | #464 | #100 | #224 | #202 | #325 |
|------------|------|------|------|------|------|
| scenario 0 | 4.41 | 4.51 | 4.56 | 6.44 | 6.45 |
| scenario 1 | 8.24 | 8.04 | 7.23 | 7.58 | 7.44 |

One obvious conclusion is that with an averaged diagram it is useless to perform an advanced simulation (with reflections for instance) since it introduces more error than precision (scenario 0 without reflection gives results closer to scenario 1).

## 8 Results

We compare cumulated density function of electric field (in V/m) in the final maps (after averaging) of each scenario. This allows to observe both the maximum value and the shape of the distribution.

### 8.1 On the ground (outdoor exposure)

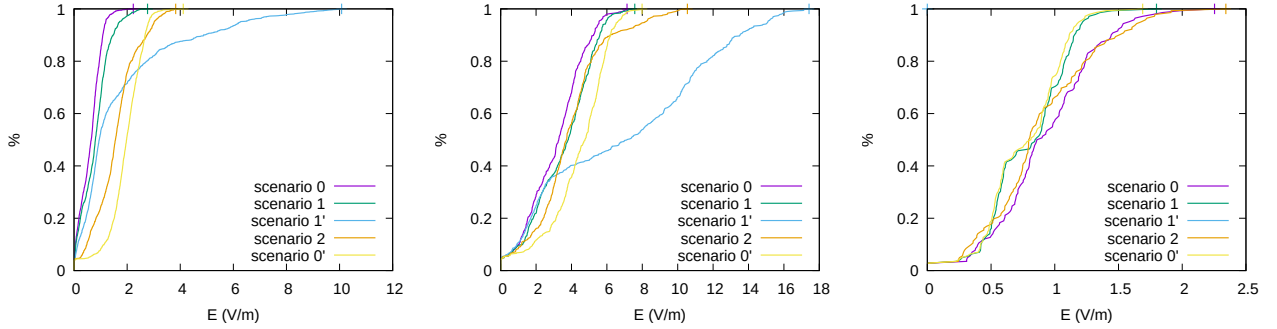


Figure 6 – Comparisons between scenarios 0, 0', 1, 1' and 2, on the ground for the three environments

### 8.2 On the facades (indoor exposure)

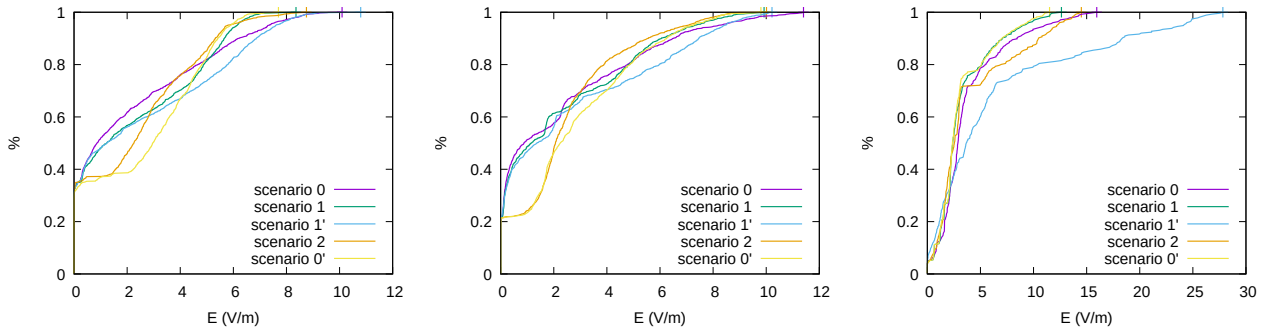


Figure 7 – Comparisons between scenarios 0, 0', 1, 1' and 2, on the facades for the three environments

### 8.3 Analysis

In all of the cases of this study, the differences between scenario 0 (*a priori* averaged diagram of all beams) and scenario 1 (*a posteriori* average of all maps, with one map per beam) are significant, both on the shape of the distribution function of the electric field, but also on the maximum exposure level. In some cases the difference can go up to 20%. The use of an average diagram, when there is a significant range of beam directions and especially changing beam shapes (with the appearance of non-negligible side lobes) has an influence on the characterization of the exposure levels. This result should be confirmed with manufacturer antenna diagrams for which attenuation values of the side lobes would be available.

Most of the time, scenario 1' (average of the maps for the beams in line of sight of the exposition areas) is a maximizing one. But it can be matched (for its maximum level) by scenario 2 in open range areas.

What mainly interests us in this study is the comparison between scenarios 0' (ANFR guidelines) and 2 (dynamic beamforming). In all the cases studied, scenario 2 gives maximum exposure levels higher or similar to scenario 0'. The usage assumptions of this study surely have a big influence on scenario 2: constant distribution of users at ground level and in buildings (this could depend on the time of day), equal service (in assigned time) among all users, continuous service (antenna at full load). However, the differences between scenarios highlight that the configuration of the antenna environment has a strong influence on the exposure levels, which is not reflected in the use of a scenario with a medium diagram as scenario 0 or 0'.

Finally this study should be carried out on a larger scale. This would make it possible to analyze the shadowed areas (exposure “ behind ” the buildings in line of sight), areas located at a greater distance from the antenna, and more complex environments with several antennas and base stations. It is important to note that the level of exposure on the facade is the level outside but that the channel was formed with users located inside buildings (taking into account attenuation by the building walls). It should be noted that the methodology implemented in this study can be deployed operationally on any site, and requires calculation resources similar to those of a conventional calculation of exposure levels (only the diagrams of antennas are changed dynamically).

## 9 Conclusion and future work

By comparing the scenarios based on the use of an average diagram (scenarios 0 and 0') with a scenario based on the average of the maps for all beams (scenario 1), it appears that, in the case of beamforming antennas, taking into account the side lobes is essential to obtain a relevant characterization of the exposure levels. This is particularly the case for an antenna having a wide horizontal angular steering capacity. This conclusion should be refined and confirmed with more complete information from the manufacturers on the diagrams of the 5G antennas that will be deployed in the field.

To make the calculation of exposure levels more precise and taking into account the antenna environment, it is possible and simple to implement in existing exposure tools a scenario which limits the focusing of the beams towards the points of exposure in line of sight of the antenna (scenario 1'). This scenario is, logically, very overestimating in the majority of the cases studied. This result justifies the use and analysis of a more advanced scenario such as the scenario integrating dynamic beamforming, taking into account the characteristics of the channel between the antenna and the users (scenario 2).

With regard to the statistical distribution of the electric field level, we also note that the scenarios based on an average diagram, including the scenario adopted for the ANFR guidelines, tend to overestimate the low electric field levels and under estimate the strong levels, compared to the scenario incorporating dynamic beamforming (scenario 2). Here again, the distribution of the electric field level shows the advantage of digital modeling which takes into account both the environment of the antenna and its realistic behavior in channel estimation. The corollary of this conclusion is that taking into account with precision the specific environment of the antenna (buildings, obstacles, etc.) for the numerical modeling of the exposure is of little interest with a simple hypothesis of a generic averaging antenna diagram.

This first study on a few sites therefore highlighted the limitations of an overly simplified statistical approach for modeling the exposure due to smart antennas. These conclusions should be supplemented by the study of larger sites, with more antennas and base stations and in larger-scale urban environments. The study could also be completed in the future with access to more complete manufacturer data, on antennas actually deployed by operators in the coming months.

## Acknowledgments

This work was partly funded by ANFR.

## 10 References

- [1] E. Degirmenci, B. Thors, and C. Törnevik, “Assessment of Compliance With RF EMF Exposure Limits: Approximate Methods for Radio Base Station Products Utilizing Array Antennas With Beam-Forming Capabilities,” *IEEE Transactions on Electromagnetic Compatibility*, vol. 58, pp. 1110–1117, Aug 2016.
- [2] B. Thors, D. Colombi, Z. Ying, T. Bolin, and C. Törnevik, “Exposure to RF EMF From Array Antennas in 5G Mobile Communication Equipment,” *IEEE Access*, vol. 4, pp. 7469–7478, 2016.
- [3] B. Thors, A. Furuskär, D. Colombi, and C. Törnevik, “Time-Averaged Realistic Maximum Power Levels for the Assessment of Radio Frequency Exposure for 5G Radio Base Stations Using Massive MIMO,” *IEEE Access*, vol. 5, pp. 19711–19719, 2017.
- [4] E. C. C. CEPT, “Analysis of the suitability of the regulatory technical conditions for 5G MFCN operation in the 3400-3800 MHz band,” tech. rep.
- [5] N. Noé, F. Gaudaire, and M. Diarra Bousso Lo, “Estimating and Reducing Uncertainties in Ray-Tracing Techniques for Electromagnetic Field Exposure in Urban Areas,” in *IEEE Conference on Antennas and Propagation in Wireless Communications*, 2013.
- [6] N. S. G. Dimic, “On Downlink Beamforming With Greedy User Selection: Performance Analysis and a Simple New Algorithm,” vol. 53, October 2015.